Chalcogenide Letters Vol. 12, No. 12, December 2015, p. 665 - 676

OPTICAL RESPONSE OF Sn DOPED Se-Te THIN FILMS

P. HEERA[a,b*], A. KUMAR[a,c], R. SHARMA[a]
[a]*Department of Physics, Himachal Pradesh University, Shimla-171005, India*
[b]*Physics Department, Govt. College, Amb, H.P. 177203, India*
[c]*Physics Department, Govt. Degree College, Kullu, H.P. 175101, India*

Optical response of Sn doped tellurium rich Se-Te thin films has been studied in the transmission range 500-3000 nm. Well-known Swanepoel's method is employed to determine the linear optical constants, i.e. refractive index (n_1), film thickness (d), absorption coefficient (α) and extinction coefficient (k), from the transmission spectra. The non-linear parameters, say nonlinear refractive index (n_{nl}) and susceptibility (χ) are obtained from the static refractive index n_0. The linear as well as the non-linear refractive indices are found to increase with an increase in Sn content. The dispersion in the refractive index has been discussed in terms of Wemple-DiDomenico single oscillator model. The optical band gap (E_g) is estimated using Tauc's extrapolation method and has been found to decrease with an increase in Sn content. The decrease in the optical band gap is ascribed to the increase in density of defect states in the valence band and increase in tailing in the conduction band. The decrease in optical band gap and increase in N/m^* ratio are consistent with increase in non-linear refractive index. Present study shows that Sn doped Se-Te glassy alloy, with high n_{nl}, can be exploited in fast optical switching devices and in high speed communication.

(Received July 26, 2015; Accepted December 7, 2015)

Keywords: Transmission Spectra, Non-linear refractive index, Dispersion, Optical band gap.

1. Introduction

Chalcogenide glasses with coordination number less than 3 are known to exhibit[1] a wide range of photostructural effects responsible for variation in refractive index and the density[2-4] of the material. Chalcogenide glasses are known to have flexible structure, in the sense that each atom can adjust its neighboring environment to satisfy the valance requirements. The optical excitations of valence electrons weaken the repulsive interactions between lone pair electrons and result in atomic displacements liable for the photostructural changes. It means that the light induced phenomena coupled with the amorphous network, having enough structure flexibility, stimulate the structural change. In early 70's the sensitivity of these glasses to light have been realized [5-7] and xerography was widely exploited[8]. These materials have received a great attention due to their interesting optical properties, such as high refractive index, large nonlinearities and low optical losses [9, 10]. The property of possessing high refractive indices ($\geq$ 3) is advantageous for strong optical field confinement, and high non linear optical susceptibility ensure their use as non linear optical elements. In addition, the large index contrast relative to air can potentially provide a complete band-gap for photonic crystal applications. Among chalcogenide glasses, Se-Te alloys have been extensively studied [11-14] due to their applications in the IR region [15-18]. Addition of metal impurities modifies the properties of binary glasses [19, 20] and helps in stabilizing the glassy matrix against the light exposure and thermal treatment [21]. Metal-chalcogenide alloys [22, 23] offer a range of optical band gaps suitable for various optical and optoelectronic applications in memory switching devices, efficient solar material and

* Corresponding author: pawanheera@yahoo.com

holographic recording systems [24]. It has been reported that the insertion of an element having large atomic mass to the binary matrix results in small glass forming region with higher transmittance in the IR region [15, 25-26]. This technological advantage prompts us to investigate the effect of Sn doping on optical properties of Se-Te system. The incorporation of Sn, heavier than Se and Te, will enhance the linear refractive index and increase the nonlinearity of the ternary system. In the literature it is reported[27] that the tellurium based glasses containing heavy elements can transmit light far in the infrared region and are able to detect CO_2 signature. Tellurium rich chalcogen glasses are found to be suitable candidate for optical limiting[28] application. In literature, Se rich Se-Te-Sn system has been studied [29, 30] extensively whereas in the present work we aim to study the optical properties of Te rich Se-Te-Sn system.

In the present work $Se_{30}Te_{70-x}Sn_x$ thin films (x= 0, 1.5, 2.5, 4.5) have been deposited on a glass substrate using vacuum thermal evaporation technique. The transmission spectra of these films, in the spectral range 500-3000nm, have been recorded at room temperature. The optical constants are evaluated using Swanepoel [31] envelope method and the optical energy gap has been estimated using famous Tauc's extrapolation method [32]. Nonlinear refractive index has been found to increase and the optical band gap is found to decrease with an increase in Sn content. Our findings are in agreement with earlier reported results.

2. Experimental details

The alloys of $Se_{30}Te_{70-x}Sn_x$ (x= 0, 1.5, 2.5, 4.5), in bulk form, were prepared by melt quenching technique. High purity (99.999%) elemental substances were weighed according to their atomic percentages and were sealed in quartz ampoules in a vacuum of 10^{-5} Torr. These ampoules were heated, one by one, in a tubular furnace to a desired temperature of 900 ^oC for 15 hours. The temperature was gradually increased, at the rate of 3- 4 ^oC/minute, from room temperature to 900 ^oC. The ampoules were rocked frequently, throughout the heating process, to ensure the proper homogenization of the melt. Once the desired temperature of 900 ^oC was obtained the ampoules were quenched in the ice cold water. The glassy alloy was separated from the ampoules by placing them in HF + H_2O_2 solution for 36 hours. Thin films of glassy alloy were deposited on the well cleaned microscopic glass substrate by the thermal vacuum evaporation technique [Vacuum coating unit HINDHIVAC 12A 4D Model] under a vacuum of 10^{-5} Torr. To achieve a film composition very near to the bulk material the films were grown at the rate of 13 Å per second. The deposition parameters for all the four films were kept identical so that the results could be compared. The films were kept inside the deposition chamber for about 24 h to achieve a metastable equilibrium. The composition of the films was checked by performing EDAX measurement using QUANTA-250, D-9393 Model. The EDAX measurements confirmed that the composition of the thin film with respect to bulk alloy approximately differ by ±6%. The amorphous nature of the bulk alloy as well as of the films was confirmed from the X-ray diffraction pattern. The transmission spectra of as-deposited thin films, in the transmission range 500 nm -3000 nm, were recorded using ultraviolet-visible-near infrared spectrophotometer [Perkin Elmer Lamda-750].

3. Results and discussion

The precise determination of the optical constants of a material is crucial for its technological applications. The obtained transmission spectra of $Se_{30}Te_{70-x}Sn_x$ thin films, reported in Fig.1, have been used to determine the optical constants. The appearance of interference fringes in the transmission spectra, due to the difference in the refractive index of the substrate and the film, ensure the optical homogeneity of the films. The optical transmittance (T) is a complex function and strongly depends on the refractive index of substrate, refractive index of the film and wavelength of the light. Fig. 1 demonstrates that the transmission spectra shift towards lower wavelength with an increase in the Sn concentration, i.e., a blue shift in the spectra is observed. An envelope through the extremes of the transmission spectra is drawn and the values for T_M,

(transmission maximum) and T_m (transmission minimum) have been recorded at different wavelengths from envelop for each spectrum.

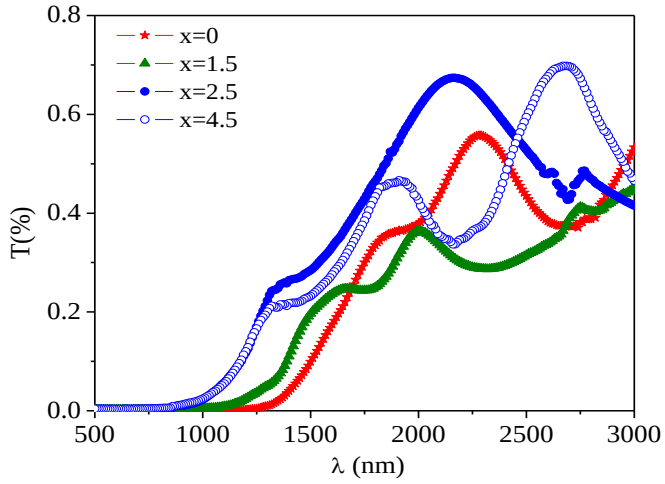

Fig.1. Variation of transmittance T (%) with wavelength λ in $Se_{30}Te_{70-x}Sn_x$ thin films.

3.1. Refractive index, film thickness, extinction coefficient:

The optical constants like refractive index (*n*), film thickness (*d*) and extinction coefficient (*k*) have been determined from well known Swanepoel envelop method. In this method the transmission envelop functions, i.e., transmission maxima T_M and transmission minima T_m, are obtained from the envelope at a particular wavelength λ_i. The refractive index in a region of absorption coefficient ($\alpha \approx 0$) is given by

$$n = \left[N + \left(N^2 - s^2 \right)^{\frac{1}{2}} \right]^{\frac{1}{2}}, \tag{1}$$

here

$$N = \frac{2s}{T_m} - \frac{s^2 + 1}{2}, \tag{2}$$

and *s* is the substrate refractive index (~1.5). For weak and medium absorption ($\alpha \neq 0$), the transmittance decreases due to the absorption and the expression for N modified as

$$N = 2s \frac{T_M - T_m}{T_M T_m} + \frac{s^2 + 1}{2} \quad , \tag{3}$$

The refractive index *n* as a function of wavelength λ for different compositions is plotted in Fig. 2. From the plot it is noticed that the refractive index decreases with an increase in the wavelength for all composition. On the other hand, *n* increases with an increase in the concentration of Sn. The decrease in the refractive index with wave length can be understood from the transmission spectra where the transmission increases with increase in wavelength. The increase in the refractive index with an increase in Sn content is attributed to the increase in density of Se-Te matrix. Addition of Sn to Se-Te matrix makes the glass dense and compact[]. The increase in refractive index can also be understood in terms of the enhanced polarizability of the material. The replacement of Te with Sn in Se-Te matrix lead to the increase in the polarizability of the material, directly proportional[33] to the refractive index of the material.

More precise values of refractive index can be obtained from the basic interference equation,

$$2nd = m\lambda, \tag{4}$$

where m is order number, it is an integer for maxima and half integral for minima in the transmission spectra. In above equation n and d represent the refractive index and thickness of the film, respectively. The thickness of the film is evaluated from the relation [34]

$$d = T_M \frac{\lambda_i \lambda_j}{2(\lambda_i n_j - \lambda_j n_i)}. \quad (5)$$

In the above equation n_i and n_j are the refractive indices at two adjacent extremes at wavelengths λ_i, and λ_j, respectively. For the two adjacent extremes T_M=1. The values of film thickness d_1

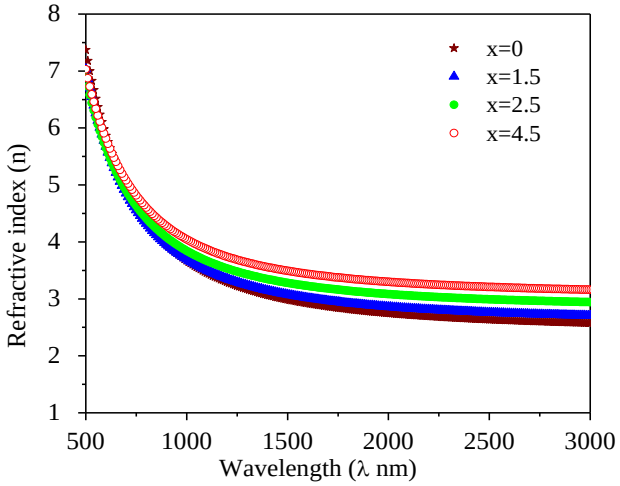

Fig.2. Variation of refractive index (n) with wavelength (λ) in $Se_{30}Te_{70-x}Sn_x$ films

along with refractive index n_1 and order number m are given in Table 1. The values d_1, n_1 and m are used to determine the order number m_0, from Eqn. (4). Using the exact value of m, the accuracy in the film thickness d_2 can be achieved significantly. Now, using the exact value of m and film thickness d_2, Eqn. (4) can be solved for n at each λ. The new values of the refractive index n_2 are fitted to the Cauchy's relation [35] i.e., $n_2=a+b/\lambda^2$, in Fig.3. The calculated values of n_2 are consistent with the Cauchy's dispersion curves that allow us to extrapolate the refractive index for all wavelengths. In Fig. 3 solid line represents Cauchy's dispersion curves and symbols represent our values of n_2.

The absorption edge of glassy materials can be divided into three regions. First, the high absorption region ($\alpha \geq 10^4$ cm^{-1}) where the transition involves in between the valance and conduction band that determines the optical band gap. The absorption coefficient for this region can be determined from the Tauc's relation [36].

The second spectral region (α = 10^2 - 10^4 cm^{-1}) is called the Urbach's exponential tail region in which absorption depends exponentially on photon energy [37]. The third region ($\alpha \leq 10^2$ cm^{-1}) involves low energy absorption and originates from defects and impurities. The absorption coefficient (α) is calculated by using the well known relation [31]

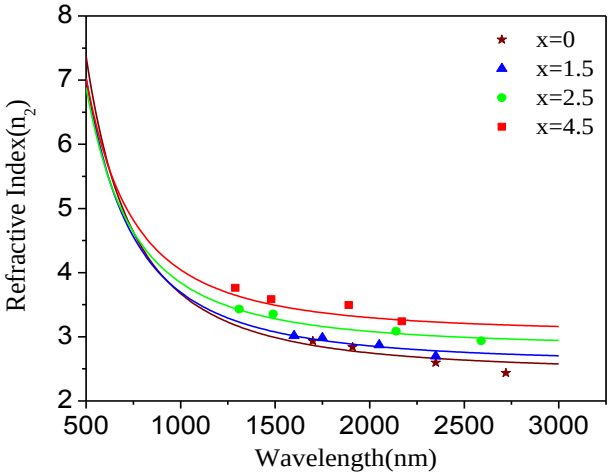

Fig.3. Variation of refractive index (n_2) with wavelength (λ) in $Se_{30}Te_{70-x}Sn_x$ thin films.

$$\alpha = \frac{1}{d} ln\left(\frac{1}{x}\right), \tag{6}$$

where x is the absorbance and d is the film thickness. The absorbance x for a material [32] is given by

$$x = \frac{E_m - \left[E_m^2 - (n^2-1)^3(n^2-s^4)\right]^{\frac{1}{2}}}{(n-1)^3(n-s^2)}, \tag{7}$$

where

$$E_m = \frac{8n^2 s}{T_m} - (n^2-1)(n^2-s^2). \tag{8}$$

The extinction coefficient (k) is a measure of loss due to scattering and absorption in the medium and can be evaluated from the relation [31]

$$k = \alpha\lambda/4\pi, \tag{9}$$

where α is the absorption coefficient and λ is wavelength. The obtained extinction coefficient is plotted in Fig. 4 that shows that the extinction coefficient decreases with an increase in Sn content at higher wavelength.

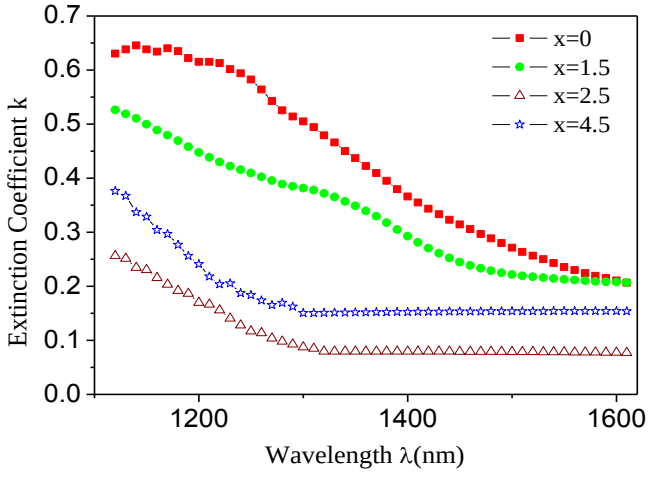

Fig.4. Variation of extinction coefficient (k) with wavelength (λ) in $Se_{30}Te_{70-x}Sn_x$ thin films

Table 1: Values of refractive index (n_1), order number (m), film thickness (d), absorption coefficient (α), optical energy gap (E_g), average energy gap (E_o), dispersion energy (E_d) and static refractive index (n_o), for $Se_{30}Te_{70-x}Sn_x$ thin films.

x	n_1 (λ= 1500 nm)	m	d_1	α (cm^{-1})	E_g (eV)	E_o (eV)	E_d (eV)	n_o
0	3.03	2.5	841.13	22724.5	1.13	2.02	10.87	2.697
1.5	3.07	2.5	678.92	18593.5	1.09	2.00	12.92	2.799
2.5	3.28	2.5	661.43	12883.1	0.91	1.88	16.13	3.011
4.5	3.49	2.0	502.23	6606.2	0.83	1.73	18.93	3.217

3.2 Optical band gap:

The optical energy gap (E_g) of $Se_{30}Te_{70-x}Sn_x$ thin films for different compositions is calculated from the absorption coefficient using Tauc's extrapolation relation [32],

$$\alpha h\nu = B\left(h\nu - E_g\right)^p, \tag{10}$$

where B is the slope of the top edge, called band tailing parameter, E_g is the optical band gap of the material and p represents the type of the transition. p= 1/2, 2, 3/2 and 3 correspond to direct allowed, indirect allowed, forbidden and indirect forbidden transitions, respectively. The variation of $(\alpha h\nu)^{1/2}$ with $h\nu$ is shown Fig. 5. The linear relationship for all the investigated samples indicates the existence of the indirect allowed transitions. The values of the optical energy gap for the indirect allowed transition are obtained from the intercept of the plot with energy axis at $(\alpha h\nu)^{1/2} = 0$. The obtained values of the optical band gap are reported in table 1. The optical band gap decreases with an increase in Sn concentration. The decrease in the optical band gap may be attributed to an increase in the density of states in the valence band. The addition of Sn creates localized states in the gap[38]. According to Mott and Davis [39] model, the width of the localized states near the mobility edges depends on the degree of disorder and defects present in the amorphous structure. Increase in Sn concentration in binary Se-Te system results in increase in localized states in the band structure that causes the band gap to decrease.

The decrease in the optical band gap can also be discussed in terms of the energy of lone pair p-orbital of chalcogen atoms. Sn, which is less electronegative, when enter the Se-Te matrix it goes into the network as a charged entity and raises the energy of some of lone-pair states thereby resulting the broadening of the valence band. As a consequence the absorption edge shift towards lower photon energy resulting into band tailing[40], responsible for decreases in the optical band gap.

3.3 Dispersion energy parameters:

The dispersion parameters play a major role in the optical communication and in designing devices for special applications. The spectral dependence of the refractive index, in visible and near infra red regions, has been analyzed using single oscillator model [41-43]. According to this model the dispersion of refractive index can be studied using the relation

$$n^2 - 1 = \frac{E_d E_o}{E_o^2 - E^2}, \tag{11}$$

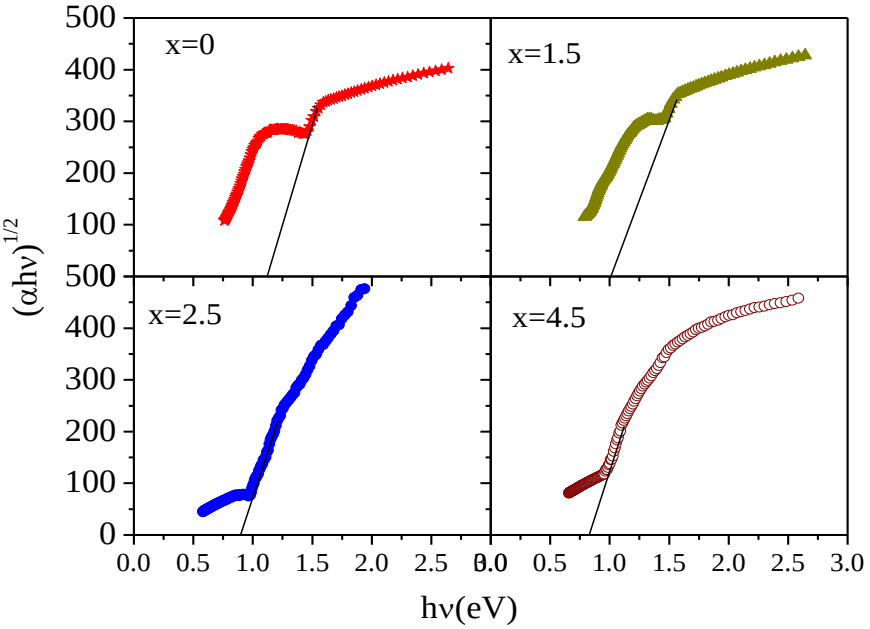

Fig.5. Variation of $(\alpha h\nu)^{1/2}$ with photon energy ($h\nu$) in $Se_{30}Te_{70-x}Sn_x$ system

where E_0 is the single effective oscillator energy or average energy gap, E_d is the dispersion energy and E is the photon energy($h\upsilon$). E_d is proportional to dielectric loss (ε) and is a measure of the average strength of inter-band transitions associated with the iconicity and the coordination number of the material. The increase in the dispersion energy is usually associated with decrease in the band gap[44]. The values of E_0 and E_d are determined from the slope $(E_0E_d)^{-1}$ and intercept (E_0/E_d) on the vertical axis in the plot $(n^2-1)^{-1}$ versus $(h\upsilon)^2$, Fig. 6, and are listed in table 1. The static refractive index (n_0) has been calculated from equation (11) in the limit $E\rightarrow 0$, i.e.,

$$n_o = \left(1 + \frac{E_d}{E_o}\right)^{1/2} \tag{12}$$

The obtained values of n_0 are listed in table 1.

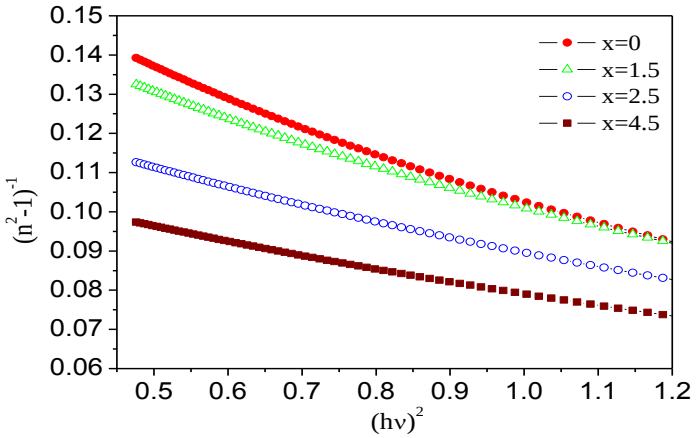

Fig. 6. $(n^2-1)^{-1}$ versus $(h\upsilon)^2$ for $Se_{30}Te_{70-x}Sn_x$ thin films.

3.4 Non-linear refractive index:

Most of the nonlinear effects originate from the nonlinear refractive index. It is observed that the chalcogenide glasses exhibit high non-linear susceptibility[45,46]. The non-linear refractive index (n_{nl}) can be expressed in terms of susceptibility [47]

$$n_{nl} = \frac{12\pi\chi^{(3)}}{n_o}, \tag{13}$$

where $\chi^{(3)}$ is third order non-linear susceptibility responsible for nonlinear phenomenon such as third harmonic generation and nonlinear refraction. The third order linear susceptibility can be written [48] as

$$\chi^{(3)} = A\left(\chi^{(1)}\right)^4 \tag{14}$$

here $\chi^{(1)}$ is linear susceptibility and is defined as $\chi^{(1)} = \frac{E_d/E_o}{4\pi}$ with A=1.7×10^{-10} e.s.u., a constant[47]. Using equation (12) $\chi^{(3)}$ can be expressed as

$$\chi^{(3)} = \frac{A}{(4\pi)^4}\left(n_o^2 - 1\right)^4 . \tag{15}$$

Obtained value of $\chi^{(3)}$ as a function of Sn concentration are plotted in Fig 7. The third order non linearity $\chi^{(3)}$ increases with an increase in Sn content whereas the optical band gap E_g decreases. This increase in $\chi^{(3)}$ is attributed to the increase in polarizability of the alloy. The calculated values of n_{nl} for the investigated samples are reported in table 2. The nonlinear refractive index n_{nl} can also be obtained from the Tauc gap, using the Moss rule $n_{nl}\ \alpha\ 1/(E_g)^4$. The obtained values of n_{nl} are much higher than the values reported [49] for other chalcogenide glasses. The increase in n_{nl} may ascribed to the increase in $\chi^{(3)}$ and decrease in E_g. The replacement tellurium with Sn, heavier than Te, causes an increase in linear refractive index and decrease in optical band gap which further results in an increase in the nonlinearity of the glass. These glasses possessing high nonlinear refractive index exhibit short response time and hence have application in fast optical switching devices and high speed signal communication.

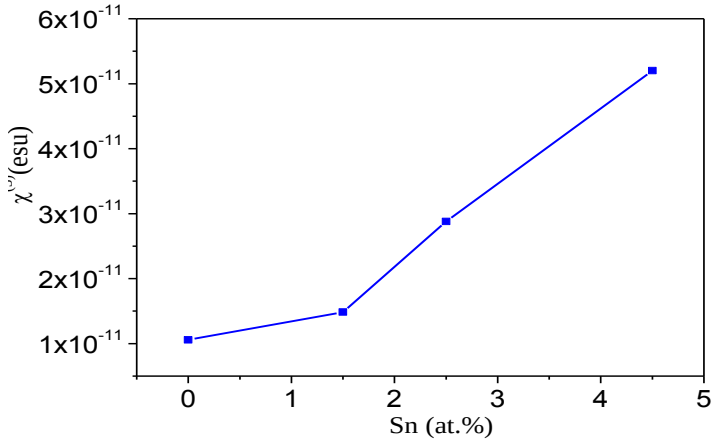

Fig.7. Variation of $\chi^{(3)}$ with Sn (at%) in $Se_{30}Te_{70-x}Sn_x$ system

3.5 Dielectric constant near the absorption edge and high frequency dielectric constant (ε_∞) :

The dielectric constant is an intrinsic property of the material [50] and it affects the movement of the electromagnetic signals through the materials. The materials with high dielectric constant will make the light to travel slowly. The complex dielectric constant (ε) of a material in

terms of the optical constants n and k is expressed as $\varepsilon = n + ik$. The real (ε') part of the dielectric constants is written[51-53] as

$$\varepsilon' = n^2 - k^2 = \varepsilon_\infty - \frac{e^2}{4\pi^2 c^2 \varepsilon_0}\frac{N}{m^*}\lambda^2 \ , \tag{16}$$

where ε_∞ is the high frequency dielectric constant, e is the charge on the electron, N is the free charge-carrier concentration, ε_o is the permittivity of free space, m^* is the effective mass of the electron and c is the velocity of light. Whereas the imaginary part can be expressed as

$$\varepsilon'' = 2nk = \frac{\varepsilon_\infty \omega_p^2 e^2}{8\pi^3 c^3 \tau}\lambda^3 \ , \tag{17}$$

where ω_p is the plasma frequency and τ is the dielectric relaxation time. Calculated values of the real (ε_∞) and imaginary (ε'') part of the dielectric constant are listed in table 2 which reveals that the real and imaginary part of the dielectric constant increases with an increasing Sn content. For k=0, in the transparent region, $\varepsilon_\infty = n^2$ and wave length dependence of ε_∞ is found to be linear as shown in Fig. 8. ε_∞ and N/m^* are determined from the slope and intercept of the fitted straight lines of ε vs λ^2 in Fig. 8 . ε_∞ and N/m^* are found to increase with an increase in Sn concentration (table 2). The increase in N/m^* ratio causes an increase in the defects states in the band structure and hence leads to the decreases in optical band gap.

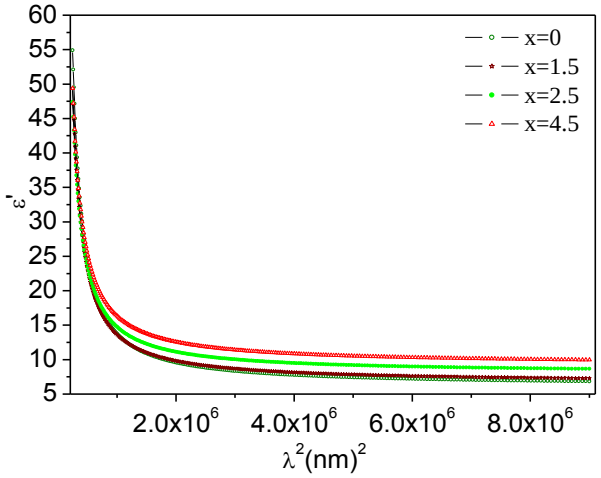

Fig.8. Variation of ε' with λ^2 for $Se_{30}Te_{70-x}Sn_x$ for x= 0, 1.5, 2.5, 4.5 thin films

3.6 Determination of the dissipation factor tan δ:

The dissipation factor (loss tangent) or loss factor can be obtained from the knowledge of the real and imaginary part of the dielectric constant and is defined as the ratio of imaginary part to the real part of the dielectric constant[54],

$$tan\delta = \varepsilon''/\varepsilon' \ , \tag{18}$$

The calculated values of the dissipation factor of the investigated films are reported in the table 2. The dissipation factor, i.e., loss increases with the Sn content.

3.7 Optical Conductivity:

The optical conductivity (σ) shows the optical response of the material and has the dimension of frequency which are valid only in Gaussian system of units. The optical conductivity of $Se_{30}Te_{70-x}Sn_x$ thin films is calculated from the relation [55]

$$\sigma = \alpha nc/4\pi \ , \tag{19}$$

where *c* is the velocity of light, α is the absorption coefficient and *n* is the refractive index. The obtained values of optical conductivity, at wavelength 850 *nm*, are given in table 2. The plot of optical conductivity (*σ*) as a function of photon energy (*hv*) is shown in Fig. 9. From the table 2, it is found that the optical conductivity increases with an increase in energy as well as in Sn content. Since *σ* is directly related to the absorption coefficient and refractive index, therefore, increase in optical conductivity may be ascribed to the large absorption coefficient and refractive index of the investigated thin films.

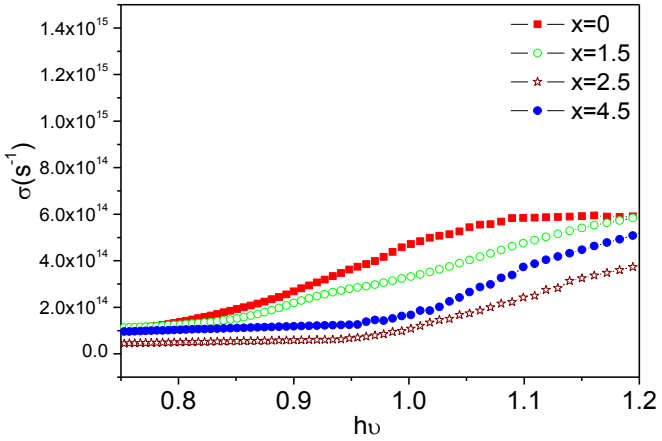

Fig.9. Variation of optical conductivity (σ) with photon energy (hv) for $Se_{30}Te_{70-x}Sn_x$ thin films.

*Table 2. Values of, dielectric constants (ε′ and ε″), optical conductivity (σ), dissipation factor Tan(δ) at λ=850 nm, high frequency dielectric constant(ε_∞), N/m*ratio and non linear refractive index (n_{nl}) for $Se_{30}Te_{70-x}Sn_x$ thin films.*

Sn (at.%)	n_{nl} x10^{-10} e.s.u	ε′	ε″	σ (s^{-1}) x 10^{14}	*Tan(δ)*	ε_∞	N/m*x10^{24} (m^{-3} Kg^{-1})
x= 0	1.477	17.316	3.791	6.69	0.218	9.366	4.05
x= 1.5	2.007	16.727	4.198	7.41	0.251	9.641	3.74
x= 2.5	3.606	17.655	4.340	7.66	0.245	10.951	3.68
x= 4.5	6.091	19.262	5.094	8.98	0.264	12.394	3.86

4. Conclusions

The Swanepoel's envelop method has been employed to determine the various optical parameters of tellurium rich $Se_{30}Te_{70-x}Sn_x$ thin films. The refractive index (*n*) is found to increase whereas extinction coefficient (*k*) decreases with an increase in Sn content. The increase in refractive index and $\chi^{(3)}$ is ascribed to the increase in density and polarizability of the material. The present results are consistent with Cauchy's dispersion relation. The dispersion of refractive index has been examined using Single oscillator (WDD) model. The dispersion parameters like dispersion energy (E_d) and static refractive index (n_0) are found to increase while average energy gap E_0 decreases. The optical band gap (E_g) estimated using Tauc's extrapolation method and is found to decrease with an increase in Sn content. This decrease in optical band gap is due to the increase in defects states in band structure and tailing of band. This finding is also supported by the increase in N/m* ratio and nonlinear refractive index n_{nl}. Present study shows that the higher value of n_{nl} in $Se_{30}Te_{70-x}Sn_x$ material enable them to be suitable candidate to fabricate as low loss optical filters, in high speed signal communication and optical limiting.

References

[1] Morigaki K, Physics of Amorphous Semiconducto, Imperial College Press, 1999.
[2] Igo T,Noguchi Y, Nagai H, Appl. Phys. Lett. **25(4)**, 193(1974).
[3] Srivastava S, Pandey V, Tripathi S K, Shukla R K, Kumar A, J. Ovonic Research **4**, 83(2008).
[4] Ahmad A, Khan S A, Sinha K,Kumar L,Khan Z H, Zulfequar M, Husain M, Vacuum **82**, 608(2008).
[5] Ovshinsky S R and Klose P H, J. Non-Cryst. Solids **8-10**, 892(1972)
[6] Tanaka K, Appl. Phys. Letters **26**, 243(1975).
[7] Tanaka K, J. Non-Cryst. Solids **35-36**, 1023(1980).
[8] Mott N F, Davis E A, Electron Process in Non-Crystalline Materials,(Clarendon Press, Oxford),1979.
[9] Van Popta A C, DeCorby R G, Haugen C J, Robinson T, McMullin J N, Opt. Express **10**, 639(2002).
[10] Harbold J, Ilday F, Wise F, Birks T, Wadsworth W, Chen Z, Opt. Lett. **27**,1558(2002).
[11] Abd-El Rahman M I, Rash M, Khafagy M, Zaki A S, Hafiz M M, Materials Science in Semiconductor Processing, **18**, 1(2014).
[12] Ahmed EL-Amin A, Mohd Badr A, Wahaab F A, Turk J. Phys **3**, 133 (2007).
[13] Kumar S, Majeed Khan M A, Chalcogenide Letters **9**(4), 145 (2012).
[14] Maged A F, Amin G A M, Semary M and Borham E, Journal of Non-Oxide Glasses **1(1)**, 53 (2009).
[15] Marquez E, Gonzalez-Leal J M, Jimenez-garay R, Vleck M, Thin Solid Films **396**, 183(2001).
[16] Pandey V, Mehta N, Tripathi S K and Kumar A, Chalcogenide Letters, **2**, 39 (2005).
[17] Sanghera J S, Florea C, Shaw L, Pureza P, Nguyen V, Bashkansky M, Dutton Z, Aggarwal I, J. Non-Cryst. Solids **354**, 462 (2008).
[18] Masahiro N, Yasuhiko A, Tsutomu S, Kazuo K, Jpn. J. Appl. Phys. **44**, 7238 (2005).
[19] Sharma P, Sharma I and Katyal S C, J. Appl. Phys. **105**, 053509 (2009).
[20] Mehta N, Sharma D, Kumar A, Physica B **391**, 108 (2007).
[21] Iovu M S, Boolchand P, Georgiev D G, Iovu S M, Popescu M Advanced Topics in Optoelectronics, Microelectronics, and Nanotechnologies II, Proc. of SPIE Vol. **5972**.
[22] Al-Ewaisi M A, Imran Mousa M A, Lafi Omar A, Kloub Mohd W, Physica B **405**, 2643 (2010).
[23] Abdel-Rahim M A, Hafiz M M, El-Nahass M M, Shamekh A M, Physica B **387**, 383 (2007).
[24] Bennouna A, Tessier P Y, Priol M, Dang Tran Q, Robin S, Phys. Stat. Sol. **117**, 51 (1983).
[25] Vasko A, Proceedings of the 11 th international congress on glass **5**, 533 (1977).
[26] Elliot S R, Physics of Amorphous Materials, 2nd edn. (Longman, London), 1991.
[27] Sun J, Nie Q, Wang X, Dai X, Zhang X, Bureau B, Boussard C, Conseil C, Ma H, Infrared Phys. Technol. **55**, 316(2012).
[28] Boudebs G, Cherukulappurath S, Guignard M, Troles J, Smektala F, Sanchez F, optics communications, **232**, 417 (2004).
[29] Saraswat V K, Kishore V, Deepika, Kananbala Sharma, Saxena N S, Sharma T P, Chalcogenide Letters **4(5)**, 61 (2007).
[30] Saraswat V K, Saxena N S, Journal of Material RRJMS **1**, 1(2012).
[31] Swanepoel R, J. Phys. E. Sci. Instrum. **17**,896 (1984).
[32] Swanepoel R, J. Phys. E. Sci. Instrum. **16**,1214 (1983).
[33] Kumar A, Heera P, Sharma P, Barman P B, Sharma R, J. Non-Cryst. Solids **358**, 3223(2012).
[34] Moss T S, Opt. Prop. Semicond. Butterworth, London, 1959.
[35] Tauc J, The Optical Properties of Solids, Amsterdam, North Holland, 1970.
[36] Abdel-Aziz M M, El-Metwally E G, Fadel M, Labib H H and Afifi M A 2001 Thin solid films **99**, 386(2000).
[37] Tauc J, Amorphous and liquid semiconductors, (Plenium Press, New York), 1979.
[38] Barreau N, Marsillac S, Bernede J C, Ben Nasrallah T, Belgacem S, Phys. Status Solid **184**, 179 (2001).

[39] Mott N F, Davis E A, Electronics processes in non-crystalline materials Oxford:Clarendon 428, 1979.
[40] Nagels P, Tichy L, Tiska A, Ticha H, J. Non-Cryst. Solids **59&60**, 1015 (1983).
[41] Wemple S H, DiDomenico M, Phys. Rev. B **3**, 1338 (197).
[42] Wemple S H, Phys. Rev. B **7**, 3767(1973).
[43] Didomenico M, Wemple S H, J. Appl. Phys. **40**, 720(1969).
[44] El-Gendy Y A, J. Phys. D: Appl.Phys. **42**,115408(2009).
[45] Smektala F, Quemard C, Couderac V, Barthelemy A, J. Non Cryst Solids, **274**, 232(2000).
[46] Quemard C, Smektala F, Couderac V, Barthelemy A, Lucas J, J. Phys. Chem. Solids **62**, 1435 (2001).
[47] Wang C, Phys. Rev. B **2**, 2045 (1970).
[48] Ticha H and Tichy L, J. Optoelectron. Adv. Mater. **4**, 381 (2004)
[49] Ogusu K, Yamasaki J and Maeda Shinpei, Optics letters **29(3)**, 265 (2004)
[50] Goswami A, Thin Film Fundamental, New Age International, New Delhi, 2005.
[51] Zemel J N, Jensen J D, Schoolar R B, Phys. Rev. A **140**, 330 (1965)
[52] Wakkad M M, Shokr E Kh, Mohamed S H, J. Non-Cryst. Solids **265**,157(2000).
[53] Fayek S A, El-Sayed S M, NDT&E Int. **39**, 39 (2006)
[54] Yakuphanoglu F, Cukurovali A, Yilmaz I, Physica B **351**, 53 (2004)
[55] Pankov J I, Optical Processes in Semiconductors, Dover, New York, 1975.